JOURNAL OF GEOPHYSICAL RESEARCH, VOL. 112, B10309, doi:10.1029/2006JB004587, 2007

Currently active regions of decelerating-accelerating seismic strain in central Asia

B. C. Papazachos,[1] E. M. Scordilis,[1] D. G. Panagiotopoulos,[1] C. B. Papazachos,[1] and G. F. Karakaisis[1]

Received 21 June 2006; revised 30 May 2007; accepted 20 July 2007; published 25 October 2007.

[1] Accelerating preshock seismic strain in a broad (critical) region and decelerating preshock seismic strain in a narrower (seismogenic) region constitute a model for intermediate-term prediction of strong main shocks. An effort is made in the present work for a forward test of the Decelerating-Accelerating Seismic Strain (D-AS) model by identifying such patterns and estimating the corresponding, probably ensuing, strong main shocks ($M \geq 7.0$) in central Asia (20°N–45°N, 42°E–105°E). Five such patterns have been identified, and the origin time, magnitude, and epicentral geographic coordinates of each of the corresponding main shocks have been estimated (predicted). Model uncertainties of the estimated time, magnitude, and space parameters of these probably ensuing main shocks, as well as appropriate statistical tests against a standard Gutenberg-Richter seismicity distribution, are also presented to allow a future objective evaluation of the model's efficiency for intermediate-term earthquake prediction.

Citation: Papazachos, B. C., E. M. Scordilis, D. G. Panagiotopoulos, C. B. Papazachos, and G. F. Karakaisis (2007), Currently active regions of decelerating-accelerating seismic strain in central Asia, *J. Geophys. Res.*, *112*, B10309, doi:10.1029/2006JB004587.

1. Introduction

[2] Prediction of individual strong earthquakes has been the ''dream'' of people in seismically active areas since antiquity. Unfortunately, short-term prediction (time uncertainty of the order of days to weeks) is not feasible at present due to the limited scientific knowledge on the physical relation between precursory phenomena and ensuing main shocks [*Wyss*, 1997]. Long-term prediction of an individual strong earthquake is not possible either, because the physical process of its generation in the fault is characterized by properties of deterministic chaos and accurate knowledge of this process is needed to predict the next strong earthquake [*Jaumé and Sykes*, 1999], which is also not available at present. It seems, however, that there is some hope for intermediate-term prediction of individual strong earthquakes (time uncertainties of the order of a few years) on the basis of precursory seismicity patterns which have predictive properties as evidenced by a wealth of reliable observations and physical interpretations provided by recently developed theories [*Evison*, 2001].

[3] Two of the most distinct such patterns are the accelerating precursory seismic strain observed in a broad (critical) region [*Tocher*, 1959; *Mogi*, 1969; *Sykes and Jaumé*, 1990; *Knopoff et al.*, 1996; *Robinson*, 2000; *Tzanis et al.*, 2000] and the seismic quiescence observed in the rupture zone (narrower seismogenic region) [*Wyss and Habermann*, 1988; *Scholz*, 1988; *Zöller et al.*, 2002; *Jaumé*, 1992; *Bufe et al.*, 1994]. The preshock seismic excitation in a broad region and the seismic quiescence in the narrower focal region of an oncoming main shock has been called ''doughnut pattern'' by *Mogi* [1969].

[4] On the basis of a damage mechanics model, *Bufe and Varnes* [1993] have proposed the following relation for the time variation of the cumulative Benioff strain, S (in $j^{1/2}$), released by accelerating preshocks at the time, t:

$$S(t) = A + B(t_c - t)^m, \quad (1)$$

where t_c is the origin time of the main shock and A, B, m are parameters determined by the available data for accelerating preshocks, with $m < 1$. *Bowman et al.* [1998] suggested the minimization of a curvature parameter, C, which is defined as the ratio of the root-mean square error of the power law (relation (1)) to the corresponding linear fit error and used this parameter to identify critical regions where intermediate magnitude preshocks occur in an accelerating mode (accelerating preshocks). Moreover, *Papazachos et al.* [2005a] proposed the application of relation (1) for decelerating Benioff strain in the narrow (seismogenic) region with $m > 1$ and they also used the curvature parameter, C, to identify seismogenic regions where intermediate magnitude preshocks occur with a decelerating mode (decelerating preshocks). This decelerating mode is formed of a transient excitation followed by continuous decrease of seismic strain.

[5] This model of accelerating generation of intermediate magnitude preshocks in a broad (critical) region and of decelerating generation of intermediate magnitude preshocks in a narrower (seismogenic) region, which follows

[1]Laboratory of Geophysics, School of Geology, Aristotle University of Thessaloniki, Thessaloniki, Greece.

0148-0227/07/2006JB004587$09.00

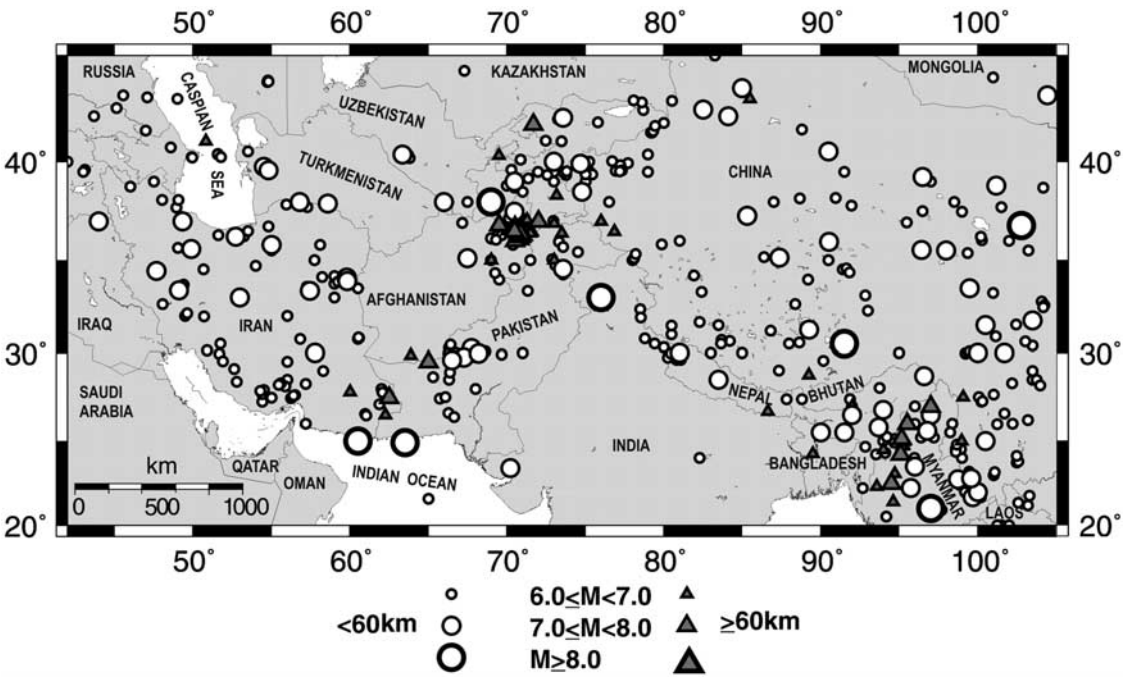

Figure 1. Map of epicenters in central Asia for the complete sample of earthquakes with M $\geq$ 6.0, which occurred between 1901 and 2005. Circles and triangles show epicenters of shallow (h < 60 km) and intermediate depth (h $\geq$ 60 km) earthquakes, respectively.

the power law relation (1) with m < 1 for accelerating preshocks and m > 1 for decelerating preshocks, has been recently further developed by including empirical relations derived by global observations which have predictive properties [*Papazachos et al.*, 2005b, 2006]. The validity of the Decelerating-Accelerating Seismic Strain (D-AS) model has been successfully tested by its application on preshock sequences of already occurred strong main shocks (M $\geq$ 6.0) in several seismotectonic regimes (Mediterranean, Himalayas, Japan, California, and South America). However, this backward procedure is not enough and forward testing by defining critical and seismogenic regions of future main shocks and attempting prediction of these main shocks is necessary for a more objective evaluation of the predictive ability of the model.

[6] Thus, in the framework of this strategy, an attempt is made in the present work to identify in central Asia critical regions, where accelerating seismic strain currently occurs, as well as narrower seismogenic regions, where decelerating seismic strain also takes place. The epicentral coordinates, magnitudes and origin times of the corresponding probably ensuing main shocks have been estimated, in order to evaluate the predicting ability of this method by a forward testing procedure.

[7] The area of central Asia considered in the present work is defined by the parallels 20°N and 45°N and meridians 42°E and 105°E. It includes Arabia, Iraq, Iran, India, western China and other countries of central Asia. Central Asia's active tectonics is mainly dominated by the convergence of the Eurasian plate with the Indian and the Arabian plates. Figure 1 shows a map of this area, where the epicenters of the earthquakes with M $\geq$ 6.0 which have occurred during the whole instrumental period (1901–2005) are plotted.

2. Relations With Predictive Properties

[8] Predictive properties of the accelerating and decelerating preshock sequences are expressed by empirically determined relations and constants, most of which have also theoretical support. Detailed information on these relations has been already published [*Papazachos et al.*, 2005b, 2006] and for this reason we only present here the relative relations and parameters for accelerating and decelerating preshock seismic sequences.

[9] An accelerating preshock sequence follows relation (1) with m < 1 and the equations

$$\log R = 0.42M - 0.30 \log s_a + 1.25 \qquad \sigma = 0.15 \qquad (2)$$

$$\log(t_c - t_{sa}) = 4.60 - 0.57 \log s_a \qquad \sigma = 0.10 \qquad (3)$$

$$M = M_{13} + 0.60 \qquad \sigma = 0.20 \qquad (4)$$

where R (in km) is the radius of the circular (critical) region (or the radius of the equivalent circle in the case of an elliptical critical region), s_a (in $j^{1/2}$ yr^{-1} 10^4 km^2) is the rate of the long- term seismic strain, t_{sa} (in years) is the start time of the accelerating sequence, t_c is the origin time of the main shock, M is the magnitude of the main shock and M_{13} is the mean magnitude of the three largest preshocks.

[10] In order to define the geometrical center of the critical (circular or elliptical) region, which corresponds to

an occurred or ensuing main shock, the broader area is separated in a grid of geographic points with certain density (e.g., 0.2°NS, 0.2°EW). For each point of the grid, the parameters of relation (1), the curvature, C, and a quality index, q_a, is calculated for a large number of assumed values of M, R, t_{sa}, t_c, e, z. The point, Q, for which the quality index, q_a, has its largest value is considered as the geometrical center of the critical region and the corresponding solution (M, R, t_{sa}, t_c, e, z) as the best solution, where e is the ellipticity and z is the azimuth of the large axis of the elliptical critical region.

[11] The quality index, q_a, is defined by the relation

$$q_a = \frac{P_a}{mC}, \tag{5}$$

where P_a is a measure of the probability that each obtained solution (M, R, t_{sa}, t_c, e, z) fits the global relations (2), (3), and (4) assuming that the deviation of each parameter follows a Gaussian distribution [*Papazachos and Papazachos*, 2001; *Papazachos et al.*, 2002]. Application of this procedure on a large sample of accelerating preshock sequences [*Papazachos and Papazachos*, 2001; *Scordilis et al.*, 2004; *Papazachos et al.*, 2005b] gave the following cutoff values for such sequences:

$$C \le 0.60,\ P_a \ge 0.45,\ m \le 0.35,\ q_a \ge 3.0. \tag{6}$$

Worldwide observations show that a mean value of m is 0.30, which is in agreement with theoretical considerations [*Rundle et al.*, 1996, 2000; *Ben-Zion et al.*, 1999] and for these reasons this value is adopted in the present work. The magnitude, M_{min}, of the smallest preshock of an accelerating preshock sequence for which relation (6) applies and q_a has its largest value is given by the relation:

$$M_{min} = 0.46M + 1.91, \tag{7}$$

where M is the magnitude of the main shock [*Papazachos et al.*, 2005b].

[12] For a decelerating preshock sequence a power law relation (1) with $m > 1$ and the following relations apply:

$$\log \alpha = 0.23M - 0.14 \log s_d + 1.40 \qquad \sigma = 0.15 \tag{8}$$

$$\log(t_c - t_{sd}) = 2.95 - 0.31 \log s_d \qquad \sigma = 0.12 \tag{9}$$

where a (in kilometers) is the large axis of the elliptical seismogenic region, M is the magnitude of the main shock, t_{sd} (in years) is the start time of the decelerating preshock sequence and s_d (in $j^{1/2}$ $yr^{-1}10^4$ km^2) is the long-term seismic strain rate (long-term seismicity) of the seismogenic region [*Papazachos et al.*, 2006]. A quality index, q_d, has been also defined in this case by the relation

$$q_d = \frac{P_d m}{C}, \tag{10}$$

where P_d is defined for a decelerating preshock sequence on the basis of the quantities α, M, t_{sd}, t_c and the relations (8) and (9), similar to P_a which has been defined on the basis of the quantities R, M, t_{sa}, t_c and relations (2), (3), and (4). The following cutoff values have been calculated by the use of global data [*Papazachos et al.*, 2006]:

$$C \le 0.60,\ 2.5 \le m \le 3.5,\ P_d \ge 0.45,\ q_d \ge 3.0. \tag{11}$$

From a large number of globally occurred decelerating preshock sequences an average value of 3.0 was derived for m and this value is adopted in the present work. It has been also shown [*Papazachos et al.*, 2006] that the following relation gives the minimum magnitude, M_{min}, of decelerating preshocks for which the best (optimum) solution is obtained:

$$M_{min} = 0.29M + 2.35, \tag{12}$$

where M is the magnitude of the main shock.

[13] The geographic point for which relations (11) hold and q_d has its largest value is considered as the geometrical center, F, of the seismogenic region and the corresponding solution (α, M, t_c, t_{sd}, e, z) as the best solution.

[14] The relations presented above are based on a large sample of globally occurred preshock sequences, which show that accelerating preshocks and decelerating preshocks of a main shock occur in partly different space and time windows, as well as for different magnitude ranges. Thus comparison of relations (2) and (8) shows that the linear dimension, R, of the critical region, where accelerating preshock strain occurs, is much larger than the linear dimension, α, of the seismogenic region, where decelerating preshock strain occurs. On the average, R, is two times larger than a and a is four times larger than the fault length of the corresponding main shock. Usually the critical region (observed acceleration) includes the complete or at least part of the seismogenic region.

[15] From relations (3) and (9) it can be deduced that the duration of the accelerating and decelerating sequences are equal for a long-term strain rate $\log s_a = \log s_d = 6.35$. Since for most areas the long-term Benioff strain rate release is usually smaller and as both sequences end at the origin time of the main shock, the accelerating sequence starts usually earlier than the corresponding decelerating sequence. Thus, for central Asia, which is investigated in the present work, where $\log s \approx 5.0$, the duration of accelerating and decelerating preshock sequences are of the order of 55 a and 25 a, respectively.

[16] From relations (7) and (12) it can be concluded that the magnitudes of the accelerating preshocks are larger than the magnitudes of the decelerating preshocks of the same main shock. Thus, for main shock magnitudes 6.0, 7.0 and 8.0, the corresponding minimum preshock magnitudes are 4.7, 5.1 and 5.6 for accelerating sequences and 4.1, 4.4 and 4.7 for decelerating sequences, respectively. It is of importance to notice that both accelerating and decelerating seismic strain patterns that precede strong main shocks ($M \ge 6.0$) are pronounced for intermediate magnitude preshocks ($M > 4.0$), for which reliable data are quite easily available nowadays. The algorithm can be applied to both circular and elliptical regions. In the present work we have used circular regions because seismic zones are not very elon-

gated in this area and the probability for including two different preshock sequences in the same critical region is relatively small for circular shapes.

[17] There are three distinct geographic points (F, V_f, P_f) which are defined by decelerating preshocks and other three points (Q, V_q, P_q) which are defined by accelerating preshocks of the same main shock (C. B. Papazachos, G. F. Karakaisis et al., Predictive properties of the Decelerating-Accelerating Seismic Strain model, submitted to *Bulletin of the Seismological Society of America,* 2007, hereinafter referred to as Papazachos et al., submitted manuscript, 2007). F and Q are the geometrical centers of the seismogenic and critical region, respectively. V_f and V_q are the geographic means of the epicenters of the decelerating and accelerating preshocks. P_f and P_q are the physical centers of the two sequences, that is, the points where the frequency of preshocks (number of preshocks per unit area) is highest and from where this frequency decays with the distance according to a power law [*Karakaisis et al.*, 2007].

[18] These six points are spatially separated in two groups. The first group is formed by the four points (F, V_f, P_f, P_q) which are at relatively short distances from the main shock epicenter and their mean distance of the their geographic mean, D (mean latitude, mean longitude) from the main shock epicenter, E, is:

$$(\mathrm{ED}) = 110 \pm 60 \text{ km}. \tag{13}$$

[19] The second group of points (Q, V_q) is located at relatively larger distances from the main shock epicenter and the distance of its mean, A, from the epicenter is given by the relation:

$$(\mathrm{EA}) = (\mathrm{DA}) + 25 \pm 80 \text{ km, for } (\mathrm{DA}) \leq 300 \text{ km}$$
$$(\mathrm{EA}) = 380 \pm 100 \text{ km, for} (\mathrm{DA}) > 300 \text{ km}. \tag{14}$$

[20] The study of a large number of preshock sequences (Papazachos et al., submitted manuscript, 2007) shows that the main shock epicenters have a tendency to delineate along the line DA and to be distributed symmetrically along this line. Thus if the distance of an epicenter from this line is considered positive when the epicenter is in the one side of this line and negative when it is in the other side, their mean distance, x, is equal to zero with a standard deviation 80 km. That is,

$$x = 0 \pm 80 \text{ km}. \tag{15}$$

[21] It has been also shown (Papazachos et al., submitted manuscript, 2007) that the quality index for decelerating and accelerating seismic strain has smaller values at the actual epicenter, E, of the main shock than at the corresponding geometrical centers F and Q ($q_{de} < q_{df}$, $q_{ae} < q_{aq}$). This has been quantitatively expressed (Papazachos et al., submitted manuscript, 2007) by the relation:

$$\frac{q_{de} + q_{ae}}{q_{df} + q_{aq}} = 0.45 \pm 0.13. \tag{16}$$

[22] Relations (13), (14), (15), and (16) can be used as constraints for the estimation (prediction) of the epicenter of an ensuing main shock.

3. Estimation of Ensuing Main Shock Parameters

[23] The main parameters of an ensuing main shock which can be estimated (predicted) on the basis of the D-AS model are: its magnitude, M, its origin time, t_c, and the geographic coordinates of its epicenter, E (φ, λ). To reliably evaluate a forward prediction, it is necessary to define in advance the model uncertainties (errors) of the parameters.

[24] The obtained best solution (M, t_c, t_{sa}), which corresponds to the geometrical center, Q, of the critical region where accelerating preshock strain takes place, provides a preliminary value for the magnitude, M, of the ensuing main shock (based on relations (2) and (4)) and for its origin time, t_c, (based on relation (3)). A second alternative for M and for t_c can be obtained from the best solution (M, t_c, t_{sd}) which corresponds to the geometrical center, F, of the seismogenic region, where decelerating preshock seismic strain takes place (based on relations (8) and (9)). In the present work we have considered the average magnitude and the average origin time values from both approaches as the predicted values for the ensuing main shock. To estimate (predict) the main shock epicenter, the relations (13), (14), (15), and (16) are applied in each geographic point of a grid (e.g., around D). For each point of the grid and each relation a probability is defined by assuming that the observed deviations from these relations have a Gaussian (normal) distribution. The average of the four probabilities for each point is considered as the representative probability of the point. The geographic point with the highest representative probability is considered as the main shock epicenter.

[25] Application of the above described procedure on preshock sequences of a large number of globally already occurred main shocks suggests that the 90% model uncertainties are equal to ±2.5 a for the origin time, ±0.4 for the moment magnitude and less than 150 km for the epicenter of a main shock. However, additional errors can be also due to false alarms, as this is indicated by tests on synthetic catalogues [*Papazachos et al.*, 2002, 2005b, 2006]. This probability for false alarms of the D-AS model has been estimated by the following procedure [*Papazachos et al.*, 2006]: The original earthquake catalogue for the Aegean area was initially declustered for its aftershocks and the Gutenberg-Richter (G-R) relation parameters were estimated for each seismic zone of this area. Assuming a G-R magnitude distribution within each zone and a random (Poisson) distribution in time, a large number of synthetic declustered (main shock) catalogues was compiled. Finally, aftershocks following typical time- and space-distribution patterns were added to evaluate the final "realistic" synthetic catalogue. Tests on a large number of synthetic catalogues by application of the D-AS model indicated a low probability (~10%) of false alarms (false presence of joint decelerating-accelerating patterns in these synthetic random catalogues).

[26] Using these two sources of errors, the joint probability for the occurrence of a main shock predicted by the D-AS model is practically 80%, if we take into consider-

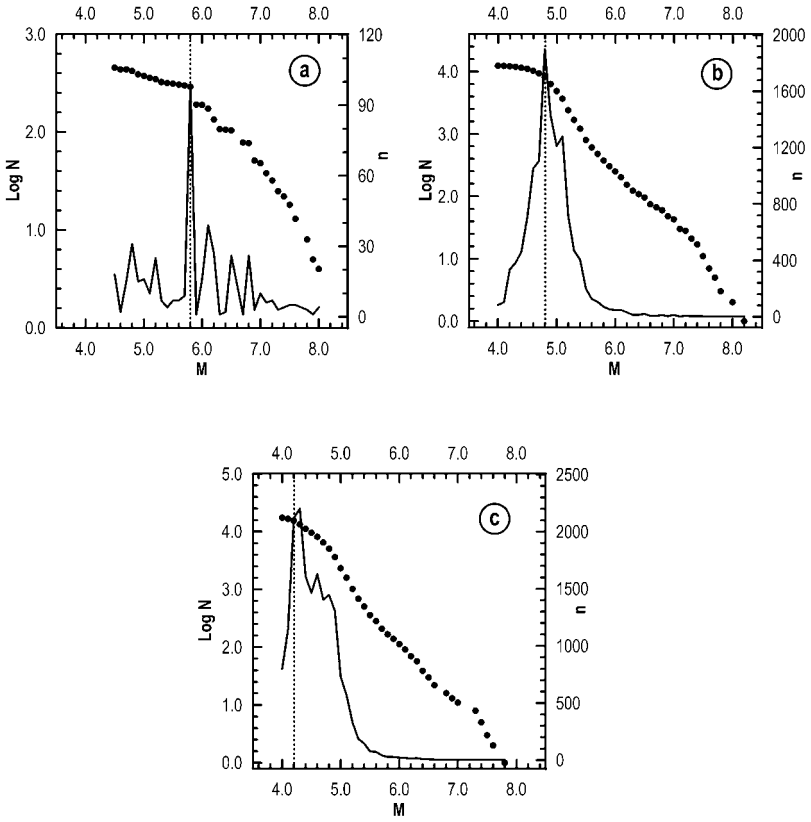

Figure 2. Frequency-magnitude and cumulative frequency-magnitude distributions for central Asia for (a) 1901–1940, (b) 1941–1990, and 1990–2005.

ation both the defined probability (90%) for model errors (based on a posteriori prediction) and the corresponding probability (90%) defined from false alarms on the basis of synthetic catalogues. This probability must be compared in each case with the probability for random occurrence of an expected main shock, which is calculated by applying the G-R recurrence law for the distribution of the magnitudes of a complete sample of shocks and assuming a standard Poisson time distribution for these shocks.

4. Data

[27] Data from international bulletins (i.e., National Earthquake Information Center, http://earthquake.usgs.gov/regional/neic/; International Seismological Centre, http://www.isc.ac.uk/search/index.html; and the Global Centroid Moment Tensor database, formerly known as the Harvard CMT catalog, http://www.globalcmt.org/CMTsearch.html) based on global and local networks have been used to compile an earthquake catalogue for the central Asia [*Scordilis et al.*, 2006]. The data of this catalogue are homogeneous with respect to magnitude, because all magnitudes are in the moment magnitude scale since magnitudes published originally in several scales (M_s, m_b, M_L, M_{JMA}, M_w) have been transformed into the moment magnitude scale, M_w(= M), by appropriate formulas [*Scordilis*, 2005, 2006]. The errors in the magnitudes of the catalogue are ~0.3 and in the location ~30 km, which are satisfactory for the purpose of the present work.

[28] The completeness of the catalogue varies from region to region but for the purpose of the present work we need to know its completeness in certain magnitude ranges and time periods for the whole area. Three complete samples of data are required for the present work. The first sample of shocks is required to calculate the long-term strain rates (s_a, s_d) needed in relations (2), (3), (8), and (9). The second sample of shocks (decelerating preshocks) is required to calculate the decelerating with time Benioff strain, while the third sample of shocks (accelerating preshocks) is required to calculate the accelerating with time Benioff strain, which are fitted by relation (1).

[29] Attempts to define a time period for which the data are complete and reliable for estimation of long-term strain rates (s_a, s_d) in several areas (Mediterranean, Japan, California, Himalayas, South America) have shown that periods which include shocks with $M \geq 5.2$ are the proper ones. For this reason this magnitude M = 5.2 has been also selected in the present case for defining the corresponding time period to calculate the long-term strain rates. Several trials have shown that this completeness requirement ($M \geq 5.2$) is fulfilled for the period 1941–2006. Figure 2a shows the frequency-magnitude and the cumulative frequency-magnitude distribution for the period 1901–1940, Figure 2b shows the same distribution for the period 1941–1990 and Figure 2c for the period 1990–2006. It is observed that for the period 1901–1940 the data are complete for $M \geq 5.8$, for the period 1941–1990 the data are complete for $M \geq 4.8$ and for the period 1990–2006 the data are complete for $M \geq 4.2$. That is, the

catalogue compiled for the whole central Asia [*Scordilis et al.*, 2006] is complete for the following periods and corresponding magnitude ranges:

$$\begin{array}{ll} 1901-1940 & M \geq 5.8 \\ 1941-1990 & M \geq 4.8 \\ 1990-2006 & M \geq 4.2 \end{array} \quad (17)$$

[30] These relations indicate that for the estimation of the long-term seismicity rates (s_a, s_d), for which data with shocks $M \geq 5.2$ are needed, the sample of data for the period 1941–2005 must be used.

[31] As we have previously discussed, the duration of accelerating preshocks in central Asia is of the order of 55 a. Since we are interesting in main shocks which will occur after 2006, we must know the completeness of the data for the period 1950–2006 to define the corresponding minimum magnitude of main shocks for which the available data allow identification of their critical region. Completeness derived for this period (1950–2006) shows that data are complete for $M_{min} = 4.8$ and using relation (7) we obtain a value of $M = 6.3$ for the minimum main shock magnitude that can be "predicted."

[32] It has been also previously mentioned that the duration of decelerating preshock sequences in central Asia is of the order of 25 a. This also suggests that we must know the completeness for the period 1980–2006 to define the minimum main shock magnitude for which the available data allow identification of seismogenic regions of main shocks expected after 2006. From the last of relation (17) and from relation (12) we observe that the completeness for the last subperiod (1990–2006), when seismic quiescence dominates in decelerating seismicity, a minimum main shock magnitude equal to 6.4 is defined. The possibility to identify seismogenic regions corresponding to main shock magnitudes $M \geq 6.4$ is not affected by the fact that during the first subperiod (1980–1989) the minimum magnitude in the available data is larger than 4.2, because during this subperiod seismic excitation, which is dominated by strong shocks (preshocks), occurs and the omission of some small shocks has no serious effect on the calculated Benioff strain. In fact, this limitation does not work in favor but against the identification of decelerating sequences, as lack of events during the first part of the decelerating period may prohibit us from correctly identifying such patterns in some cases.

[33] Although the data completeness allows the identification of both critical and seismogenic regions corresponding to main shocks with $M \geq 6.4$ in central Asia, we have limited the present investigation to main shocks with $M \geq 7.0$, in order to increase the accuracy of the sample of data used and because several of the earthquakes with $M < 7.0$ in this area are associated shocks (aftershocks, foreshocks, etc).

[34] The size of the data sample depends on the dimension of the region considered (critical, seismogenic), which increases with increasing main shock magnitude (see relations (2) and (8)). Application on already occurred earthquakes and tests on synthetic catalogues suggest that a sample of at least 20 shocks (preshocks) is necessary to obtain reliable results and limit the number of false alarms. The data used for the predictions performed in the present work span the period until 30 September 2006.

5. Results

[35] The whole area of central Asia (20°N–45°N, 42°E–105°E) has been separated in a grid of geographic points with high density (0.2°NS, 0.2°EW). For each grid point the parameters C, P_d, and q_d were calculated and those points which fulfilled relation (11) were considered as possible geometrical centers of seismogenic regions where decelerating seismic strain occurs. These points were geographically clustered in five groups. The point of each group for which q_d has its largest value has been considered as the geometric center, F, of the seismogenic region where decelerating seismic strain currently occurs and the corresponding solution (M, t_c, C, q_d, a, $logs_d$, M_{min}, n, t_{sd}) was considered as the best solution. By the same procedure five corresponding critical regions were defined where accelerating seismic strain currently occurs and the corresponding solution was considered as the best solution.

[36] The parameters (M, t_c, C, q, a, logs, M_{min}, n, t_s) of the best solution for each of the five cases are given in Table 1. The first of the two lines in each case gives the parameters of the seismogenic (decelerating preshock) region, while the second one corresponds to the parameters of the critical (accelerating preshock) region. In the first column the two estimated values of the origin time, t_c, are listed, while in the third column the two values of the estimated magnitude, M, are also presented. In the second column of Table 1 the geographic coordinates of the center of the seismogenic region, F(φ, λ), and of the critical region, Q(φ, λ), are given.

[37] Figure 3 shows on corresponding maps the epicenters of the decelerating shocks (dots), the epicenters of the accelerating shocks (small open circles), the circular seismogenic region (which includes epicenters of decelerating shocks) and the circular critical region (which includes epicenters of accelerating shocks). The numbers (1, 2, 3, 4, 5) correspond to the five code numbers of Tables 1 and 2. The corresponding time variations of the cumulative Benioff strain for decelerating and accelerating shocks are also shown, along with the best fit curves that fit the data according to the power law relation (1) with $m = 3.0$ for decelerating strain and $m = 0.3$ for accelerating strain.

[38] In Table 2 the estimated (predicted) origin time, t_c, magnitude, M, and epicenter coordinates, E(φ, λ), for each of the five probably ensuing main shocks are given. The origin time and magnitude listed in Table 2 for each of the five probably ensuing main shocks are the average of the corresponding two values of t_c and M listed in Table 1. The epicenter coordinates, E(φ, λ), listed in Table 2 for each of the probably ensuing main shocks have been estimated by the previously described procedure. The focal depths of these main shocks are expected to be $h \leq 100$ km.

[39] For the uncertainties of the estimated time, magnitude and location of the probably ensuing main shocks we have adopted the model uncertainties ±2.5 a for the origin time, ±0.4 for the magnitude, and ≤150 km for the epicenter of the expected main shock. As previously mentioned, the probability for the occurrence of a main shock predicted by this model is ~80%, if we take into consider-

Table 1. Parameters of the Circular Region of Decelerating Seismic Strain and of the Circular Region of Accelerating Seismic Strain[a]

Seismic Strain	t_c	φ, λ	M	R/α, km	C	q	M_{min}	n	t_s	Log s, $j^{1/2}$ yr^{-1} 10^4 km^2
					Case 1					
Decelerating	2007.9	45.3, 46.9	7.6	317	0.25	11.7	4.5	121	1974	4.58
Accelerating	2009.2	42.0, 49.0	7.1	546	0.49	6.6	5.2	116	1950	4.97
					Case 2					
Decelerating	2007.9	33.8, 55.0	7.2	207	0.26	11.3	4.3	25	1987	5.26
Accelerating	2010.3	38.5, 55.5	7.2	537	0.41	6.4	5.2	107	1958	5.05
					Case 3					
Decelerating	2009.0	40.0, 61.0	7.8	309	0.22	12.9	4.5	56	1985	5.05
Accelerating	2009.7	40.0, 63.3	8.0	1215	0.44	7.4	5.7	148	1959	5.08
					Case 4					
Decelerating	2010.7	36.5, 82.4	7.4	253	0.28	9.8	4.4	74	1988	5.15
Accelerating	2009.8	36.5, 80.4	7.6	712	0.34	4.6	5.5	98	1976	5.28
					Case 5					
Decelerating	2010.0	23.7, 97.0	7.7	294	0.18	14.1	4.5	242	1989	5.24
Accelerating	2010.0	19.0, 97.3	7.2	392	0.37	6.2	5.1	81	1953	4.99

[a]Here t_c is the estimated origin time for the expected main shock; φ, λ are the geographic coordinates of the geometrical center of the region; M is the magnitude of the expected main shock; α is the radius of the region; C is the curvature parameter; q is the quality index; M_{min} is the magnitude of the smallest shock (preshock); n is the number of these shocks; t_s is the start year of the sequence; and logs is the mean long-term strain rate in each region.

ation the model errors (based on a posteriori predictions) and the possibility of false alarms (false presence of joint decelerating-accelerating patterns) indicated by applications of the model in synthetic but realistic random catalogues [*Papazachos et al.*, 2006]. The calculated probability for random occurrence of each one of the expected five main shocks, in the predicted time, magnitude and space windows, as this is calculated from the typical seismicity level of each area, assuming a G-R relation, are equal to 0.01, 0.05, 0.01, 0.01, 0.19, respectively, that is, much smaller than the probability (0.8) predicted by the D-AS model.

6. Information for an Objective Evaluation of Predictions

[40] In the present work all scientific information is given for an objective backward evaluation of the predictions made in this paper after the expiration of the estimated time windows (e.g., 2013). This information concerns the method applied, the predicted parameters (epicenter coordinates, origin time, magnitude) and their uncertainties, the probability for the occurrence of the earthquakes in the defined space, time and magnitude windows as well as the probability for random occurrence of each earthquake in these windows. An accurate definition of the broader area which has been searched for the identification of the D-AS pattern is also made (20°N–45°N, 42°E–105°E). Thus the occurrence or nonoccurrence of such strong main shocks in regions of the broad area where no such pattern has been identified can be also considered for the evaluation. However, for the application of any scientifically valid procedure of evaluation, additional information and tests are necessary.

[41] The present paper deals with predictions of large main shocks ($M \geq 7.0$). The D-AS model has (in principle) the ability to predict only the largest earthquake (main shock) of a clustered in space and time seismic sequence which also includes other (associated) shocks (preshocks, aftershocks). Associated shocks cannot be predicted by the described procedure because their preshock region and preshock time cannot be identified, as they are parts of the preshock region and time of the main shock. In some (rare) cases associated shocks are comparable in size with the main shock and their epicenter, origin time and magnitude can also lie within the predicted space, time and magnitude windows. Therefore the generation of at least one earthquake with: focal depth $h \leq 100$ km, observed epicenter within a circle of radius 150 km, centered at the predicted epicenter, observed magnitude equal to the predicted magnitude ±0.4 and origin time the predicted origin time ±2.5 a will be considered as a success. The nongeneration of a predicted earthquake within these space, time and magnitude windows will be considered as a failure. The generation of an earthquake with $M \geq 7.0$ and $h \leq 100$ km in any part of the investigated broader area of central Asia within the time windows (e.g., until 2013) but outside the five predicted space windows will be also considered as a failure.

Figure 3. Information on the present decelerating-accelerating seismic strain in the five regions of central Asia. Dots are epicenters of decelerating shocks, which are included in the smaller circular (seismogenic) region, and very small open circles are epicenters of accelerating shocks, which are included in the larger circular (critical) region. The numbers correspond to case numbers of Tables 1 and 2, where information on the calculated parameters is presented. The corresponding time variations of the decelerating and accelerating Benioff strain, S, are also shown next to each map. Solid lines correspond to best fit curves using the power law relation (1).

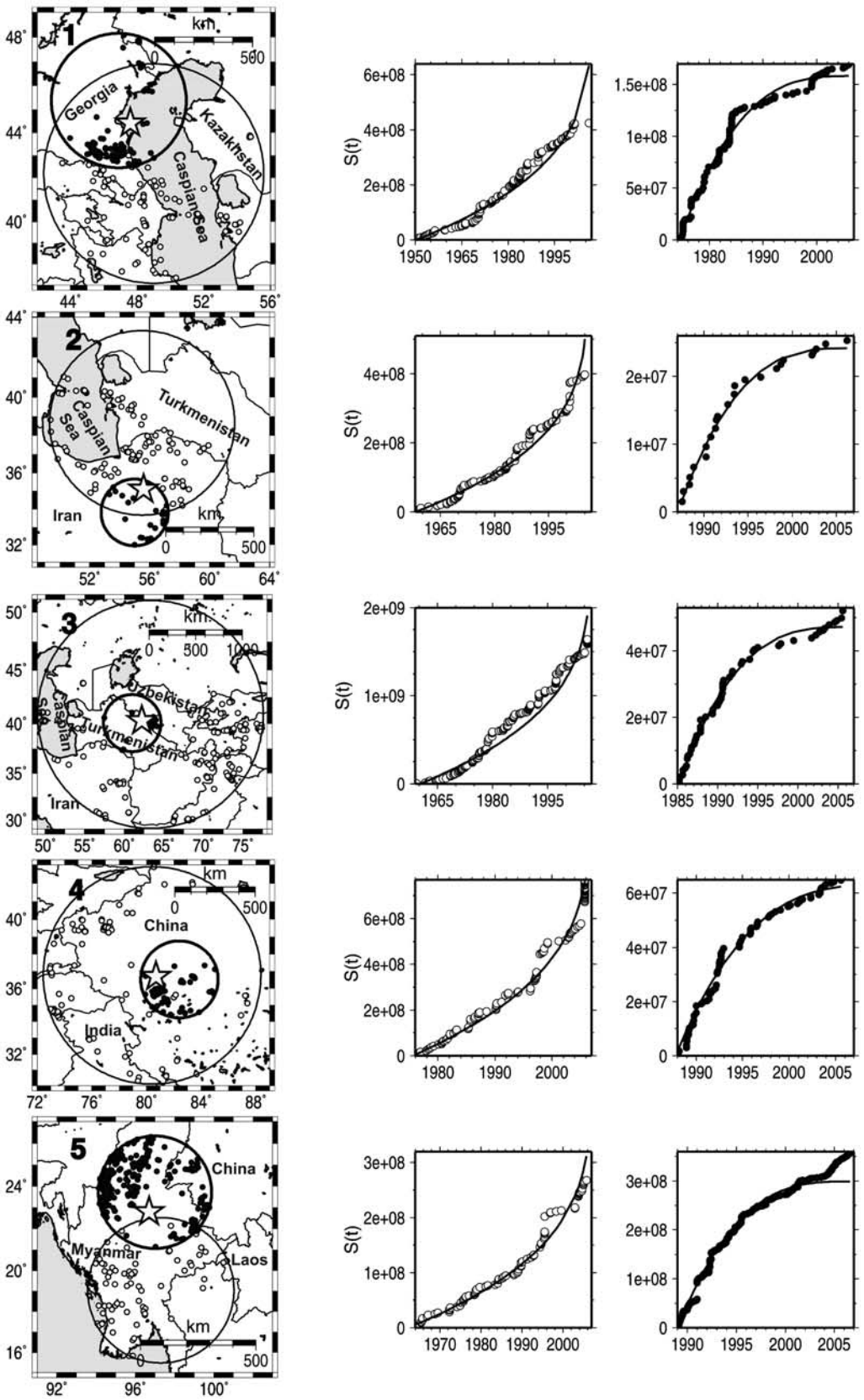
1
Georgia
Kazakhstan
Caspian Sea
km
0
500
2
Caspian Sea
Turkmenistan
Iran
3
Uzbekistan
Turkmenistan
Caspian Sea
Iran
4
China
India
5
China
Myanmar
Laos
S(t)

Figure 3

Table 2. Predicted Origin Time t_c, Epicenter Coordinates E, and Magnitude M for Each of the Five Probably Ensuing Main Shocks in Central Asia[a]

Case	Area	t_c	E, φ, λ	M
1	northern Caspian Sea	2008.6	44.4°N, 47.6°E	7.3
2	southern Caspian Sea	2009.1	35.1°N, 55.6°E	7.2
3	northeast of Iran	2009.4	40.3°N, 62.2°E	7.9
4	Tibet	2010.3	36.7°N, 80.7°E	7.5
5	northern Myanmar	2010.0	22.8°N, 96.7°E	7.4

[a]Model uncertainties are: ±2.5 a for the origin time, ≤150 km for the epicenter, ±0.4 for the magnitude, and focal depth h ≤100 km for each expected main shock, with an ∼80% probability.

[42] The information given in the present work also allows designing appropriate tests for the objective evaluation of the presented predictions. For example, we can consider as a simple quantitative measure of the evaluation a success ratio defined as the ratio of the sum of the number of the success cases to the sum of all (success and failure) cases. This ratio in the case of complete failure (none of the five predicted earthquakes occurs within the predicted windows) takes a zero value. In case of complete success (all five predicted main shocks occurred and no main shock with $M \geq 7.0$ occurred in the broad searched area) this ratio is equal to 1. If, for example, two of the predicted main shocks occur and a main shock with $M \geq 7.0$ occurs in the broader search area, outside of the five predicted regions the proposed success ratio takes a value equal to 2/6 (=0.33).

[43] However, the information contained in the present work also allows to apply alternative quantitative statistical tests, which will facilitate future evaluation of the results. A large number of tests to evaluate the efficiency of predictions and false alarms is available in the literature, such as the relative operating characteristic (ROC) and error diagrams [*Molchan*, 1990; *Molchan and Kagan*, 1992; *Joliffe and Stephenson*, 2003] or likelihood methods [e.g., *Kagan and Knopoff*, 1977; *Bevington and Robinson*, 1992; *Gross and Rundle*, 1998; *Kagan and Jackson*, 2000; *Rhoades and Evison*, 2006]. Since the prediction window in the present study (end of catalogue, October 2006, to end of last prediction window, June 2012, i.e., 7.75 a) is relatively large, we have applied the tests described by *Kagan and Jackson* [1995]. For this purpose we have used the 5 regions for which strong earthquakes have been predicted and separated the remaining area in 40 random bins. For each of the 40 random bins outside the prediction areas the G-R probability of occurrence of a $M > 7.0$ within a period of 7.75 a (prediction period) is ∼9.2%.

[44] To perform the tests, we have to define the probabilities of occurrence, p_i ($i = 1,\ldots,45$), for each of the 45 zones (5 prediction circles and 40 bins for background area). For the proposed D-AS model and for the 5-a prediction window, we used the previously mentioned probability of 80% within the 5 circles and 20% of the G-R probability for the remaining 40 bins, as this can be considered as an appropriate choice for the 20% of cases not covered by the D-AS model. For the remaining 2.75 a of the complete examined period, we used the corresponding G-R probabilities. On the other hand, for the G-R model, which was used for comparison, we have employed the corresponding G-R probabilities for the five prediction areas and the 9.2% probability for the 40 bins of the remaining area.

[45] All tests were implemented by performing 5000 simulations: for each simulation a uniform random number between 0 and 1 was drawn and compared with against p_i; if that number was less than the zone probability, p_i, (for each model) then the zone is considered filled ($c_i = 1$), otherwise it is considered empty ($c_i = 0$). Detailed information for all performed tests can be found in the work of *Kagan and Jackson* [1995]. We should also point out that the combination of D-AS probabilities (80%) for the 5-a period in each prediction area with the 2.75-a G-R probabilities practically did not affect the 80% probability estimate, as the corresponding G-R probabilities are much smaller, with the exception of case 5 in Table 1, where the combined probability increases to ∼91.5%.

[46] The first test, called N test, corresponds simply to the total number of expected main shocks for each model, using the 5000 simulations. The corresponding cumulative probability plot is shown in Figure 4a, where the D-AS and G-R models are presented with a solid and dashed line, respectively. The two curves show a small difference, as is verified by the expected number of earthquakes also plotted in this figure for each model. It is interesting to note that the D-AS model predicts ∼4.9 events until 2012.5, whereas the G-R model predicts 4.1 events. This comparison is quite interesting, as the probabilities for the individual 45 zones examined are completely different. However, when summed up, the obtained estimates are comparable, showing that the 80% probability used does not lead to unrealistic assumptions and that the expected ∼8-a behavior for both models is compatible regarding the total number of $M > 7.0$ events expected. On the other hand, the relatively small differences between the two curves of Figure 4a show that it will not be possible to perform a reliable discrimination of the model performance at the end of the examined period, if the total number of occurred events is used as the single evaluation criterion.

[47] The second test, called L test [*Martin*, 1971], computes the logarithm of likelihood, defined as

$$L = \sum_{i=1}^{N} c_i \log p_i + \sum_{i=1}^{N} (1 - c_i) \log(1 - p_i). \qquad (18)$$

[48] The significance of L is clear: If zones with high probability ($p_i \gg 0$) are filled ($c_i = 1$) and zones with low probability ($1 - p_i \gg 0$) are empty ($c_i = 0 \rightarrow 1 - c_i = 1$), then L obtains large values, showing the significance of the specific probability distribution and corresponding hypothesis. On the contrary, low L values suggest a poor model performance. Unfortunately, for both models (D-AS and G-R), the corresponding curves were almost identical, similar to the N test, suggesting that this test is also not adequate for a future model evaluation. For this reason, we employed the R test [*Martin*, 1971], where the difference $R = L_1 - L_2$ is estimated. L_1 and L_2 are the computed log likelihoods from equation (18) for the probability distributions (p_i, $i = 1,\ldots,45$) of the two models. Following the approach of *Kagan and Jackson* [1995], in Figure 4b we present two R curves, one (solid line) computed using the c_i values from the synthetic catalogues compatible with

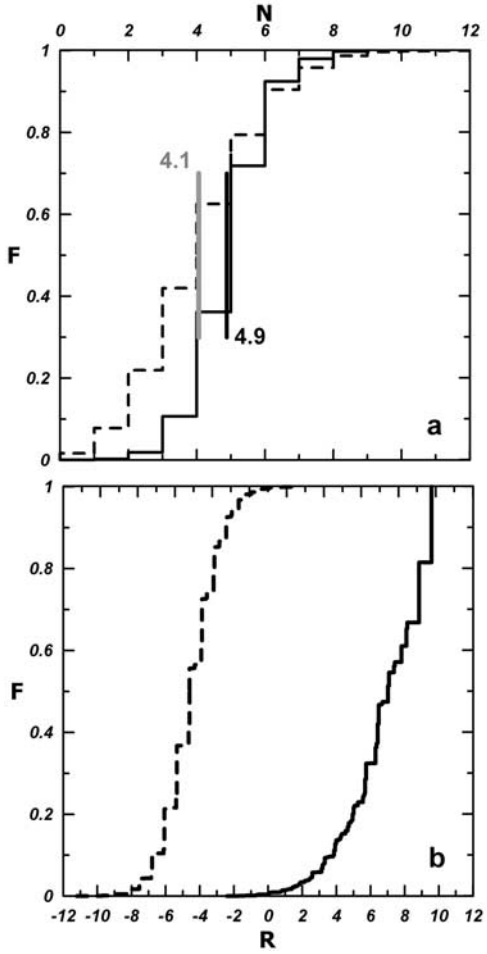

Figure 4. (a) Plot of the cumulative curves of the expected number of main shocks N and (b) the difference of log likelihoods R for the probability distributions and synthetic catalogues of the D-AS and G-R models (see section X for an explanation). The mean number of events expected in the next ~8 a according to each model is also shown in Figure 4a. Notice the significant difference of the two R curves, depending on the assumed probabilities used to create the synthetic catalogues, which will allow the evaluation of the performance of both models after the end of the prediction period.

the D-AS probabilities and one (dashed line) computed using the synthetic catalogues compatible with the G-R probabilities. The two R curves show a completely different pattern, with no overlapping at the 95% confidence level. The reason for this difference is clear: in the five zones where large earthquakes are expected according to the D-AS model, G-R probabilities are very small. On the other hand, in each of the 40 background seismicity bins, the D-AS probabilities are very small (20% of the corresponding G-R ones). As a result, the difference of likelihoods in each zone, is significant and strongly depends on the assumed probability model. Therefore the corresponding R values that will be determined from the finally observed $M > 7.0$ main shock distribution until 2012.5 will allow to completely quantitatively evaluate the reliability of the proposed prediction approach.

7. Discussion

[49] Although the model applied in the present work is based on observationally derived relations, most properties of the model have received theoretical support. This support concerns basic physical models which predict accelerating and decelerating seismic strain, as well as theoretical predictions of observed values for parameters of relations and constants.

[50] Several attempts have been made to physically interpret accelerating seismic strain on the basis of physical models. The most widely used of these models are the Critical Earthquake Model [*Sornette and Sornette*, 1990; *Allègre and Le Mouël*, 1994; *Sornette and Sammis*, 1995; *Rundle et al.*, 2000] and the Stress Accumulation Model [*Bowman and King*, 2001; *King and Bowman*, 2003; *Mignan et al.*, 2006]. According to the first one, the earthquake generation process is considered as a critical phenomenon culminated in a large event (main shock), which is considered as a critical point. For the second model, stress owing to creep at depth and slip on adjacent faults is accumulated in the fault regions of an ensuing main shock and is estimated by the back-slip, which is required to move a fault with parameters (strike, dip, rake, displacement) those of the fault of the main shock. Recent results show that observational properties of accelerating seismicity can be explained by both models (Papazachos et al., submitted manuscript, 2007). Thus a power law for the time variation of seismic strain (relation (1)) is also expected both by the Critical Earthquake Model [*Sornette and Sammis*, 1995], as well as by the Stress Accumulation Model [*Mignan*, 2006].

[51] Decelerating seismic strain can be attributed to the physical process predicted by the Stress Accumulation Model. Thus a stress shadow at some distance from the fault, with additional decrease of the dimension of the shadow region with time predicted by this model, is also in good agreement with recently observational properties of decelerating seismic strain (Papazachos et al., submitted manuscript, 2007).

[52] Relation (2) and its scaling coefficients (0.42, −0.30) are in excellent agreement with the corresponding relation and its scaling coefficients (0.43, −0.33) derived theoretically by *Dobrovolsky et al.* [1979] using a soft-inclusion elastic model for the seismogenic region. Furthermore, the value 0.3 of the exponent m of relation (1), derived from a large number of observations [e.g., *Zöller and Hainzl*, 2002; *Papazachos et al.*, 2005b] is also in very good agreement with theoretical considerations and laboratory results which suggest values of m between 0.25 and 0.33 [*Ben-Zion et al.*, 1999; *Guarino et al.*, 1999; *Rundle et al.*, 2000; *Ben-Zion and Lyakhovsky*, 2002].

[53] Prediction of an individual earthquake is a very difficult scientific problem. The model applied in the present work seems to be promising for intermediate-term prediction, since it has been successfully backward tested by its application on preshock sequences of several complete samples of strong ($M \geq 6.0$) main shocks located in a variety of seismotectonic regimes (west Mediterranean,

Adriatic, Aegean, Anatolia, Himalayas, Japan, California) [*Papazachos et al.*, 2005b, 2006]. This model has been also successfully applied for the prediction of a recent large earthquake (8 January 2006, M = 6.9, Cythira Island) in the western part of the Hellenic Arc [*Papazachos et al.*, 2007]. We can therefore conclude that the D-AS model can be considered as promising for improving techniques of time-dependent seismic hazard assessment. For example, preparedness measures can be focused on regions which are candidates for the generation of strong earthquakes, in order these measures to be effective and financially feasible. The model, however, needs further forward testing in order to better define its abilities and limitations and the present work is part of this testing procedure.

[54] By using data which concern preshock sequences of forty six main shocks with magnitudes between 6.3 and 8.3 that occurred in a variety of seismogenic regimes (Papazachos et al., submitted manuscript, 2007) it has been shown that the quality index of both accelerating, q_a, and decelerating, q_d, sequences varies with the time to the main shock. In the early stage, when the sequence is identified, the value of the quality index is small ($q \approx 3.0$) and then it increases continuously until a few years ($\sim$3 a) before the generation of the main shock, when it takes its largest value, and then decreases continuously up to generation of the main shock. This observation suggests that the predicting ability of the model applied in the present work follows the same time pattern. Thus, after the identification of a D-AS pattern, the region must be continuously monitored and the parameters of the expected main shock must be reevaluated at regular time intervals.

[55] **Acknowledgments.** The authors would like to thank D. D. Bowman, an anonymous reviewer, and the Associate Editor of *Journal of Geophysical Research* for their constructive comments and suggestions, which helped to improve the manuscript. We also thank P. Wessel and W. H. F. Smith [*Wessel and Smith*, 1995] for freely distributing the GMT software that was used to produce some of the figures of the present study.

References

Allègre, C. J., and J. L. Le Mouël (1994), Introduction of scaling techniques in brittle failure of rocks, *Phys. Earth Planet. Inter.*, *87*, 85–93.

Ben-Zion, Y., and V. Lyakhovsky (2002), Accelerated seismic release and related aspects of seismicity patterns on earthquake faults, *Pure Appl. Geophys.*, *159*, 2385–2412.

Ben-Zion, Y., K. Dahmen, V. Lyakhovsky, D. Ertas, and A. Agnon (1999), Self-driven mode switching of earthquake activity on a fault system, *Earth Planet. Sci. Lett.*, *172*, 11–21.

Bevington, P. R., and D. K. Robinson (1992), *Data Reduction and Error Analysis for the Physical Sciences*, 2nd ed., 328 pp., McGraw-Hill, New York.

Bowman, D. D., and G. C. King (2001), Accelerating seismicity and stress accumulation before large earthquake, *Geophys. Res. Lett.*, *28*, 4039–4042.

Bowman, D. D., G. Quillon, C. G. Sammis, A. Sornette, and D. Sornette (1998), An observational test of the critical earthquake concept, *J. Geophys. Res.*, *103*, 24,359–24,372.

Bufe, C. D., S. P. Nishenko, and D. J. Varnes (1994), Seismicity trends and potential for large earthquakes in Alaska-Aleutian region, *Pure Appl. Geophys.*, *142*, 83–99.

Bufe, C. G., and D. J. Varnes (1993), Predictive modeling of seismic cycle of the greater San Francisco Bay region, *J. Geophys. Res.*, *98*, 9871–9883.

Dobrovolsky, J. P., S. I. Zubkov, and B. J. Miachkin (1979), Estimation of the size of earthquake preparation zones, *Pure Appl. Geophys.*, *117*, 1025–1044.

Evison, F. F. (2001), Long-range synoptic earthquake forecasting: An aim for the millennium, *Tectonophysics*, *333*, 207–215.

Gross, S., and J. B. Rundle (1998), A systematic test of time-to-failure analysis, *Geophys. J. Int.*, *133*, 57–64.

Guarino, A. S., S. Ciliberto, and A. Garcimartin (1999), Failure time and microcrack nucleation, *Europhys. Lett.*, *47*, 456–461.

Jaumé, S. C. (1992), Moment release rate variations during the seismic circle in the Alaska-Aleutians subduction zone, in *Proceedings of the Wadati Conference on Great Subduction Earthquakes*, edited by D. Christensen et al., pp. 123–128, Univ. of Alaska Fairbanks, Fairbanks.

Jaumé, S. C., and L. R. Sykes (1999), Evolving towards a critical point: A review of accelerating seismic moment/energy release rate prior to large and great earthquakes, *Pure Appl. Geophys.*, *155*, 279–306.

Joliffe, I. T., , and D. B. Stephenson (Eds.) (2003), *Forecast Verification: A Practitioner's Guide in Atmospheric Science*, 240 pp., John Wiley, Hoboken, N. J.

Kagan, Y. Y., and D. D. Jackson (1995), New seismic gap hypothesis: Five years after, *J. Geophys. Res.*, *100*, 3943–3959.

Kagan, Y. Y., and D. D. Jackson (2000), Probabilistic forecasting of earthquakes, *Geophys. J. Int.*, *143*, 438–453.

Kagan, Y. Y., and L. Knopoff (1977), Earthquake risk prediction as a stochastic process, *Phys. Earth Planet. Inter.*, *14*, 97–108.

Karakaisis, G. F., C. B. Papazachos, D. G. Panagiotopoulos, E. M. Scordilis, and B. C. Papazachos (2007), Space distribution of preshocks, *Boll. Geofis. Teorica Appl.*, in press.

King, G. C. P., and D. D. Bowman (2003), The evolution of regional seismicity between large earthquakes, *J. Geophys. Res.*, *108*(B2), 2096, doi:10.1029/2001JB000783.

Knopoff, L., T. Levshina, V. J. Keilis-Borok, and C. Mattoni (1996), Increased long-range intermediate-magnitude earthquake activity prior to strong earthquakes in California, *J. Geophys. Res.*, *101*, 5779–5796.

Martin, B. R. (1971), *Statistics for Physicists*, 209 pp., Elsevier, New York.

Mignan, A. (2006), The stress accumulation model, Ph.D. thesis, 219 pp., Inst. de Phys. du Globe de Paris, Paris.

Mignan, A., D. D. Bowman, and G. C. P. King (2006), An observational test of the origin of accelerating moment release before large earthquakes, *J. Geophys. Res.*, *111*, B11304, doi:10.1029/2006JB004374.

Mogi, K. (1969), Some features of the recent seismic activity in and near Japan: II. Activity before and after great earthquakes, *Bull. Earthquake Res. Inst. Univ. Tokyo*, *47*, 395–417.

Molchan, G. M. (1990), Strategies in strong earthquake prediction, *Phys. Earth Planet. Inter.*, *61*, 84–98.

Molchan, G. M., and Y. Y. Kagan (1992), Earthquake prediction and its optimization, *J. Geophys. Res.*, *97*, 4823–4838.

Papazachos, B. C., G. F. Karakaisis, C. B. Papazachos, and E. M. Scordilis (2007), Evaluation of the results for an intermediate term prediction of the 8 January 2006 Mw = 6.9 Cythera earthquake in southwestern Aegean, *Bull. Seismol. Soc. Am.*, *97*, 347–352.

Papazachos, C. B., and B. C. Papazachos (2001), Precursory accelerating Benioff strain in the Aegean area, *Ann. Geofis.*, *144*, 461–474.

Papazachos, C. B., G. F. Karakaisis, A. S. Savvaidis, and B. C. Papazachos (2002), Accelerating seismic crustal deformation in the southern Aegean area, *Bull. Seismol. Soc. Am.*, *92*, 570–580.

Papazachos, C. B., E. M. Scordilis, G. F. Karakaisis, and B. C. Papazachos (2005a), Decelerating preshock seismic deformation in fault regions during critical periods, *Bull. Geol. Soc. Greece*, *36*, 1490–1498.

Papazachos, C. B., G. F. Karakaisis, E. M. Scordilis, and B. C. Papazachos (2005b), Global observational properties of the critical earthquake model, *Bull. Seismol. Soc. Am.*, *95*, 1841–1855.

Papazachos, C. B., G. F. Karakaisis, E. M. Scordilis, and B. C. Papazachos (2006), New observational information on the precursory accelerating and decelerating strain energy release, *Tectonophysics*, *423*, 83–96.

Rhoades, D. A., and F. F. Evison (2006), The EEPAS forecasting model and the probability of moderate-to-large earthquakes in central Japan, *Tectonophysics*, *417*, 119–130.

Robinson, R. (2000), A test of the precursory accelerating moment release model on some recent New Zealand earthquakes, *Geophys. J. Int.*, *140*, 568–576.

Rundle, J. B., W. Klein, and S. Gross (1996), Dynamics of a traveling density wave model for earthquakes, *Phys. Rev. Lett.*, *76*, 4285–4288.

Rundle, J. B., W. Klein, D. L. Turcotte, and B. D. Malamud (2000), Precursory seismic activation and critical point phenomena, *Pure Appl. Geophys.*, *157*, 2165–2182.

Scholz, C. H. (1988), Mechanism of seismic quiescences, *Pure Appl. Geophys.*, *126*, 701–718.

Scordilis, E. M. (2005), Globally valid relations converting M_S, m_b and M_{JMA} to M_w, paper presented at Conference on Earthquake Monitoring and Seismic Hazard Mitigation in Balkan Countries, NATO, Borovetz, Bulgaria, 11–17 Sept.

Scordilis, E. M. (2006), Empirical global relations converting Ms and mb to moment magnitude, *J. Seismol.*, *10*(2), 225–236, doi:10.1007/s10950-006-9012-4.

Scordilis, E. M., C. B. Papazachos, G. F. Karakaisis, and V. G. Karakostas (2004), Accelerating seismic crustal deformation before strong main

shocks in Adriatic and its importance for earthquake prediction, *J. Seismol.*, *8*, 57–70.

Scordilis, E. M., C. B. Papazachos, G. F. Karakaisis, and B. C. Papazachos (2006), A catalogue of earthquakes in central Asia for the period 1901–2005, Pub. Geophys. Lab., Univ. of Thessaloniki, Thessaloniki, Greece.

Sornette, A., and D. Sornette (1990), Earthquake rupture as a critical point: Consequences for telluric precursors, *Tectonophysics*, *179*, 327–334.

Sornette, D., and C. G. Sammis (1995), Complex critical exponents from renormalization group theory of earthquakes: Implications for earthquake predictions, *J. Phys. I*, *5*, 607–619.

Sykes, L. R., and S. Jaumé (1990), Seismic activity on neighboring faults as a long term precursor to large earthquakes in the San Francisco Bay area, *Nature*, *348*, 595–599.

Tocher, D. (1959), Seismic history of the San Francisco bay region, *Spec. Publ. Calif. Div. Mines Geol.*, *57*, 39–48.

Tzanis, A., F. Vallianatos, and K. Makropoulos (2000), Seismic and electrical precursors to the 17-1-1983, M = 7 Kefallinia earthquake, Greece, signatures of a SOC system, *Phys. Chem. Earth Part A*, *25*, 281–287.

Wessel, P., and W. H. F. Smith (1995), New version of generic mapping tools, *Eos Trans. AGU Electron. Suppl.*, Aug. 15. (Available at http://www.agu.org/eos_elec/95154e.html)

Wyss, M. (1997), Cannot earthquakes be predicted?, *Science*, *278*, 487–488.

Wyss, M., and R. E. Habermann (1988), Precursory seismic quiescence, *Pure Appl. Geophys.*, *126*, 319–332.

Zöller, G., and S. Hainzl (2002), A systematic spatiotemporal test of the critical point hypothesis for large earthquakes, *Geophys. Res. Lett.*, *29*(11), 1558, doi:10.1029/2002GL014856.

Zöller, G., S. Hainzl, J. Kurths, and J. Zschau (2002), A systematic test on precursory seismic quiescence in Armenia, *Nat. Hazards*, *26*, 245–263.

G. F. Karakaisis, D. G. Panagiotopoulos, B. C. Papazachos, C. B. Papazachos, and E. M. Scordilis, Laboratory of Geophysics, School of Geology, Aristotle University of Thessaloniki, Thessaloniki GR-54124, Greece. (kpapaza@geo.auth.gr)